

Which π -clamped conjugated monocycles exhibit ring currents?

Remco W. A. Havenith,^a Leonardus W. Jenneskens,^{*b} Patrick W. Fowler^{*c} and Alessandro Soncini^c

^a Department of Chemistry, University of Warwick, Coventry, UK CV4 7AL

^b Debye Institute, Department of Physical Organic Chemistry, Utrecht University, Padualaan 8, 3584 CH Utrecht, The Netherlands. E-mail: jennesk@chem.uu.nl; Fax: +31-30-2534533; Tel: +31-30-2533128

^c Department of Chemistry, University of Exeter, Stocker Road, Exeter, UK EX4 4QD. E-mail: P.W.Fowler@exeter.ac.uk; Fax: +44-1392-263434; Tel: +44-1392-263466

Received 26th January 2004, Accepted 10th March 2004

First published as an Advance Article on the web 1st April 2004

Quenching/survival of ring currents in π -clamped conjugated monocycles is controlled by the match or mismatch in parity between the frontier orbitals of the central π -conjugated $4n+2/4n$ monocycle and those of the clamps. Changes in ring current are *not* primarily caused by bond alternation or 'Mills–Nixon' effects; current and geometry changes on clamping are both consequences of electronic structure.

Introduction

The correspondence between $4n+2/4n$ π -electron counts and diatropic/paratropic ring currents in planar Hückel monocycles stems from their characteristic frontier-orbital structure.¹ Using the *ipsocentric* partition of total ($\sigma + \pi$) current density into orbital contributions,² it can be shown that the induced currents in the monocycles are dominated by HOMO–LUMO virtual excitations, and hence can be ascribed to just *four* of the $4n+2$ π -electrons in the diatropic case, and to *two* of the $4n$ π -electrons in the paratropic case.¹ As part of the exploration of the concept of aromaticity, synthetic chemists have sought for many years to subvert the Hückel rules and to make unconventional monocycles by altering their natural geometries. Benzene rings with strong bond alternation, *e.g.* **1**³ and **2**,⁴ and planarised cyclooctatetraene (COT), *e.g.* **6**,⁵ have been produced using a "clamping" strategy, where annelation is used to impose the desired geometric constraints (Scheme 1). In this way, systems with positive and negative 'Mills–Nixon effects',⁶ *i.e.*, positive and negative bond length differences, $\Delta R = R_1 - R_2$ have been devised (see also Scheme 1).

As explicit mapping of current density shows, ring currents survive in some of these novel clamped systems but not in others; in **2** the characteristic diatropic benzene ring current remains strong whereas it is quenched in **1** and in the tris(cyclobutadieno)-clamped model **4**;⁷ in **6** and **7** the paratropic ring current expected on the basis of the Hückel $4n$ rule is indeed found, but is then predicted to disappear in the COT analogue of **4**, *e.g.* *exo*-**8**.⁸ This variety of behaviour has a ready explanation in the orbital model based on the *ipsocentric* approach: the survival/quenching of currents in functionalised^{7–9} and constrained¹⁰ systems such as **1–4** and **6–8**, is rationalised by considering the extent to which the HOMO and LUMO of the central ring remain intact, preserving the character of the dominant virtual excitation(s). Annelation with saturated moieties, as in **2**, **6**, and the related model systems containing cyclobutano clamps (**3**^{7,9} and **7**⁸) leaves the π HOMO and π^* LUMO of the monocycle essentially undisturbed and, hence, preserves the diatropic/paratropic current. On the other hand, annelation with strongly interacting unsaturated moieties inserts new π and π^* levels into the gap, changes the set of active virtual excitations and, hence, destroys the current (Fig. 1). This quenching effect has been demonstrated computationally for **1**, **4** and its *exo*-COT analogue **8**.^{7–9}

Our subject here is another clamping group that frequently features in discussions of aromaticity: the *unsaturated* 3,4-di-

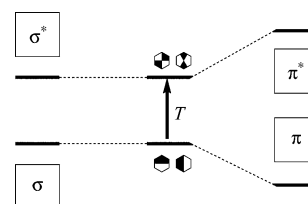


Fig. 1 The effect of clamping on the electronic structure of benzene and 1,3,5,7-cyclooctatetraene (COT). In benzene and COT itself the ring current arises from a translationally (T) allowed HOMO–LUMO vertical excitation, and a rotationally (R) allowed HOMO–LUMO vertical excitation, respectively.² When saturated groups are attached (left), this transition is undisturbed, as the extra (usually σ) orbitals from the clamping group lie outside the active π space, but when unsaturated groups are attached (right), other magnetically active orbitals often intrude into the frontier region. The present paper discusses a case where *no* π intruder orbitals are in fact present.

methylenecyclobuteno unit.^{6,11,12} Although this group is π -conjugated, the predicted bond alternation for tris(3,4-dimethylenecyclobuteno)benzene (**5**, Scheme 1) is comparable to that in tris(cyclobutano)benzene (**3**) where the clamping group is saturated, and the computed nucleus-independent chemical shift (NICS) value (*ca.* -10 ppm,¹²) in **5** indicates little change in the magnetic character of the central ring, compared to benzene itself. This appears to pose a problem for our rationalisation of currents in terms of a saturated/unsaturated dichotomy.^{7–9} How does this clamping group fit with the scheme presented in Fig. 1?

The present paper reports calculations of current maps for tris(3,4-dimethylenecyclobuteno)benzene (**5**) and the COT analogues *endo*-**9** and *exo*-**10** (Scheme 1), which lead to a generalisation of the survival/quenching criteria. It is shown that pictorial molecular orbital theory explains these *ab initio* results and gives a concise predictive rationalisation of the effects of the different π and σ clamping groups on magnetic properties.

Computational details

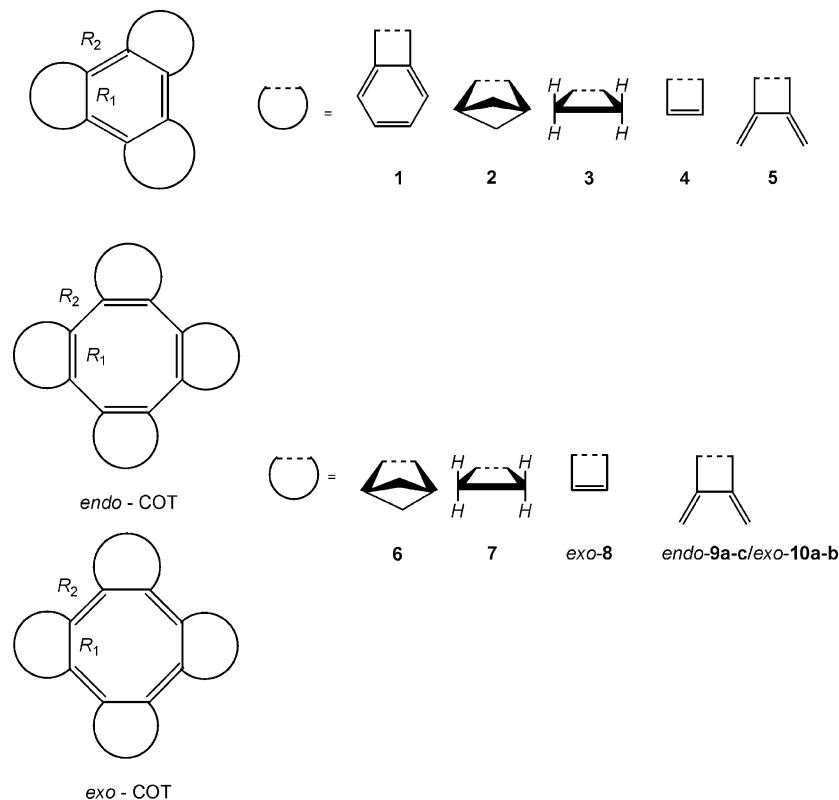
Geometries

Geometries were optimised at the RHF/6-31G** level of theory using GAMESS-UK.¹³ Under the constraint of D_{3h} symmetry, tris(3,4-dimethylenecyclobuteno)benzene (**5**) was found to be a true minimum, as shown by a Hessian calculation (Table 1). In the case of tetrakis(3,4-dimethylenecyclobuteno) COT, there are two conceivable valence isomers denoted *endo* (**9**) or *exo*

Table 1 Computed geometric and energetic data for clamped benzene **5** and COT systems **9a–c** and **10a–b** (see Scheme 1)

Compound	R_1^a [Å]	R_2^a [Å]	ΔR^a [Å]	ΔE_r^b [kJ mol ⁻¹]	N_{imag}^c	$\Delta E_{\text{HOMO-LUMO}}^d$ [eV]	j_{max} [au]
5 (D_{3h}) ^e	1.405	1.377	0.028	—	0	9.66 ($3e'' \rightarrow 4e''$)	0.067
<i>endo-9a</i> (D_{4h})	1.359	1.459	-0.100	48.99	4 ^f	6.62 ($2b_{2u} \rightarrow 2b_{1u}$)	0.121
<i>endo-9b</i> (D_4)	1.356	1.456	-0.100	36.23	1 ^f	6.64 ($10b_2 \rightarrow 11b_1$)	0.125
<i>endo-9c</i> (D_{2d})	1.349	1.455	-0.106	0.00	0	7.51 ($12a_1 \rightarrow 9a_2$)	0.065
<i>exo-10a</i> (D_{4h})	1.504	1.328	0.176	16.82	5 ^f	6.45 ($2b_{1u} \rightarrow 2b_{2u}$)	0.097
<i>exo-10b</i> (D_4)	1.500	1.326	0.174	8.45	0	6.44 ($11b_1 \rightarrow 10b_2$)	0.096

^a RHF/6-31G** carbon-carbon bond lengths; $\Delta R = R_1 - R_2$ (see also Scheme 1). Similar results were obtained at the B3LYP/6-31G** level of theory. ^b RHF/6-31G** ΔE_r values with respect to *endo-9c*: $E_{\text{tot}} = -917.842429$ au. ^c Number of imaginary frequencies at stationary point. ^d RHF/6-31G** HOMO-LUMO gap. ^e RHF/6-31G**, **5**: $E_{\text{tot}} = -688.397785$ au. ^f Imaginary-frequency modes: *endo-9a* [102.3i, 90.9i (twofold degenerate) and 64.5i], *endo-9b* (23.9i), and *exo-10a* [88.5i, 73.4i (twofold degenerate), 35.8i and 25.6i].

**Scheme 1**

(**10**) on the basis of double-bond positions with respect to the clamps (Scheme 1),¹⁴ which are visualised separately as individual maps.¹⁰ Optimisation of **9** under full planar D_{4h} symmetry gave the high-order saddle point **9a**. Upon relaxation, a non-planar transition state of D_4 symmetry (**9b**) and a true minimum of D_{2d} symmetry (**9c**) were identified (Table 1). Optimisation of the *exo*-isomer **10** under full planar D_{4h} symmetry gave again a high-order saddle point (**10a**), which relaxed to a true minimum of D_4 symmetry (**10b**) lying only 8.45 kJ mol⁻¹ above **9c** (Table 1). Details of relative energies are given in Table 1.

Magnetic properties

The σ -, π - and total ($\sigma + \pi$) current densities induced by a unit magnetic field acting along the principal axis were computed and mapped for **5**, **9a–c** and **10a–b** using the *ab initio* CTOCD-DZ (continuous transformation of origin of current density-diamagnetic zero) method¹⁵ in the 6-31G** basis set with the SYSMO¹⁶ program and at the RHF/6-31G** geometries. The ipsocentric² character of this method leads to a natural partition of the total current density into physically distinct orbital contributions, which can also be visualised as maps. For the

planar geometries, the maps are plotted in a plane 1 a_0 above the central ring, close to the maximum π density, where the current flow is effectively parallel to the molecular plane. Contours denote modulus of current density, and vectors represent in-plane projections of the current. For the non-planar geometries, the plotting plane lies 1 a_0 above the molecular median plane. In all plots, diatropic circulation is shown *anti*-clockwise and paratropic circulation clockwise.

Results

Fig. 2 shows the total ($\sigma + \pi$) induced current density in the plotting plane for **5** (D_{3h}), the contribution of the full set of π orbitals, and from the HOMO $3e''$ pair alone. It is seen that the system supports a diatropic ring current, concentrated on the central ring, arising from circulation of the π electrons and dominated by the mobility of just four HOMO electrons. In other words, **5** exhibits the classic magnetic characteristics of unperturbed benzene. In the plotting plane the π current has a maximum intensity j_{max} 0.067 au, to be compared with 0.08 au for benzene⁹ itself calculated in the same approach; π currents within the unsaturated 3,4-dimethylenecyclobuteno clamping

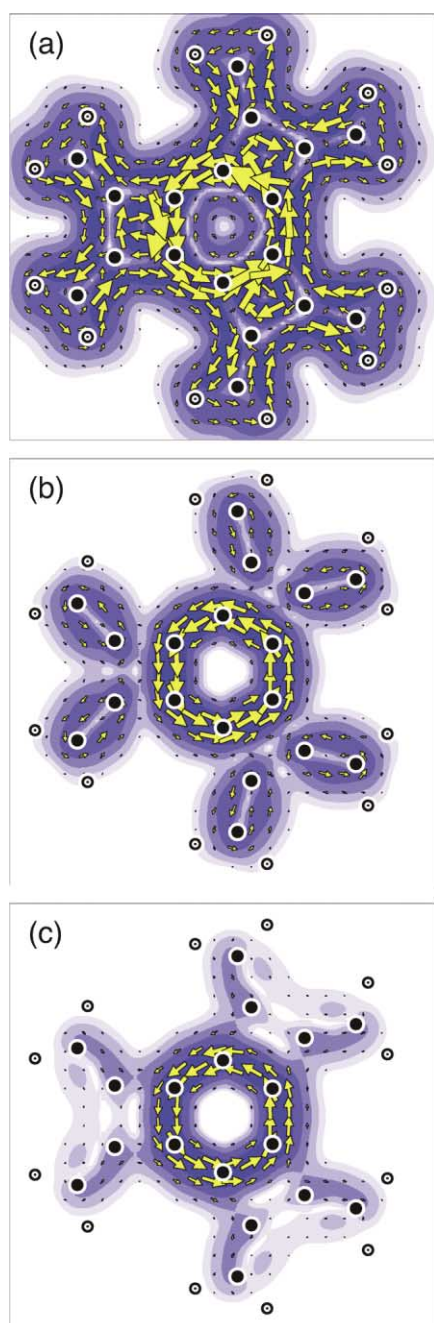


Fig. 2 CTOCD-*DZ/6-31G**//RHF/6-31G*** current density maps for **5** (D_{3h}); (a) total ($\sigma + \pi$), (b) π -only and (c) $3e'$ HOMO contribution: carbon ● and hydrogen ○.

groups are localised and weak, as they are in the free 3,4-dimethylenecyclobutene valence isomer of benzene.¹⁷

Fig. 3 shows, for the planar D_{4h} geometry of the *endo*-valence isomer of tetrakis(3,4-dimethylenecyclobuteno) COT (*endo-9a*), the total ($\sigma + \pi$) induced current density in the plotting plane, the contribution of the full set of π orbitals, and from the non-degenerate $2b_{2u}$ HOMO alone. It is seen that the system supports a paratropic ring current, concentrated on the central ring, arising from circulation of the π electrons and dominated by the mobility of just the two HOMO electrons. The maps for the *exo*-valence isomer (*exo-10a*) are not shown here as they are generally similar in all respects. Thus, in planar form, **9a** and **10a** exhibit the magnetic characteristics of a delocalised, planar D_{4h} 8π -electron COT monocycle. In the plotting plane, the π current has maximum intensities j_{\max} 0.121 au (*endo-9a*) and 0.097 au (*exo-10a*), to be compared with 0.130 au for planar D_{4h} COT itself.⁸ The smaller current density in *exo-10a* is consistent with previous results for planar angle-constrained [$a(\text{CCH}) =$

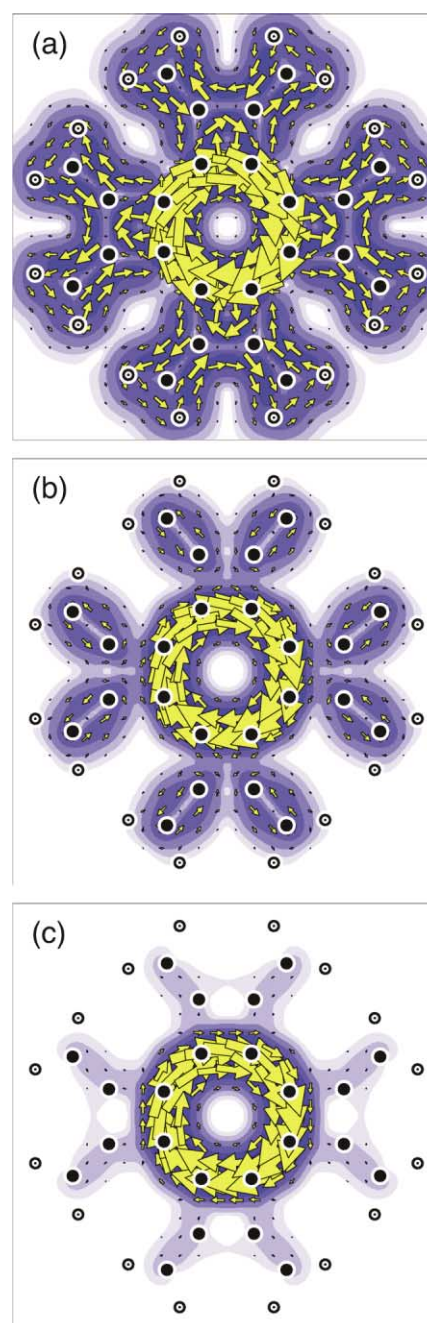


Fig. 3 CTOCD-*DZ/6-31G**//RHF/6-31G*** current density maps for *endo-9a* (D_{4h}); (a) total ($\sigma + \pi$), (b) π -only and (c) $2b_{2u}$ HOMO contribution: carbon ● and hydrogen ○.

90°] COT for which also an *endo*- (j_{\max} 0.250 au) and *exo*- (j_{\max} 0.070 au) valence isomer were found ($\Delta E_{\text{endo} - \text{exo}} = 202 \text{ kJ mol}^{-1}$).¹⁰ Again, π currents within the clamping groups are localised and weak.

Furthermore, it turns out that loss of planarity does not affect the essentials of the maps. Fig. 4 shows the total induced current density in the plotting plane and the contribution of the non-degenerate HOMO for the two non-planar local minima *exo-10b* (D_4) and *endo-9c* (D_{2d}). As the plotting plane now cuts some peripheral bonds, the total induced current density maps show extra features in this region, but the ring currents remain essentially identical with those of the planar forms [in the central region j_{\max} 0.096 au (*exo-10b*) and 0.065 au (*endo-9c*)]. Significantly, in both cases the current is still attributable almost entirely to the two electrons of the π -derived HOMO. The paratropic current survives at the global minimum geometry, *endo-9c*. This current exists in spite of the tub-like conformation of the COT ring in **9c**. Free COT has a localised

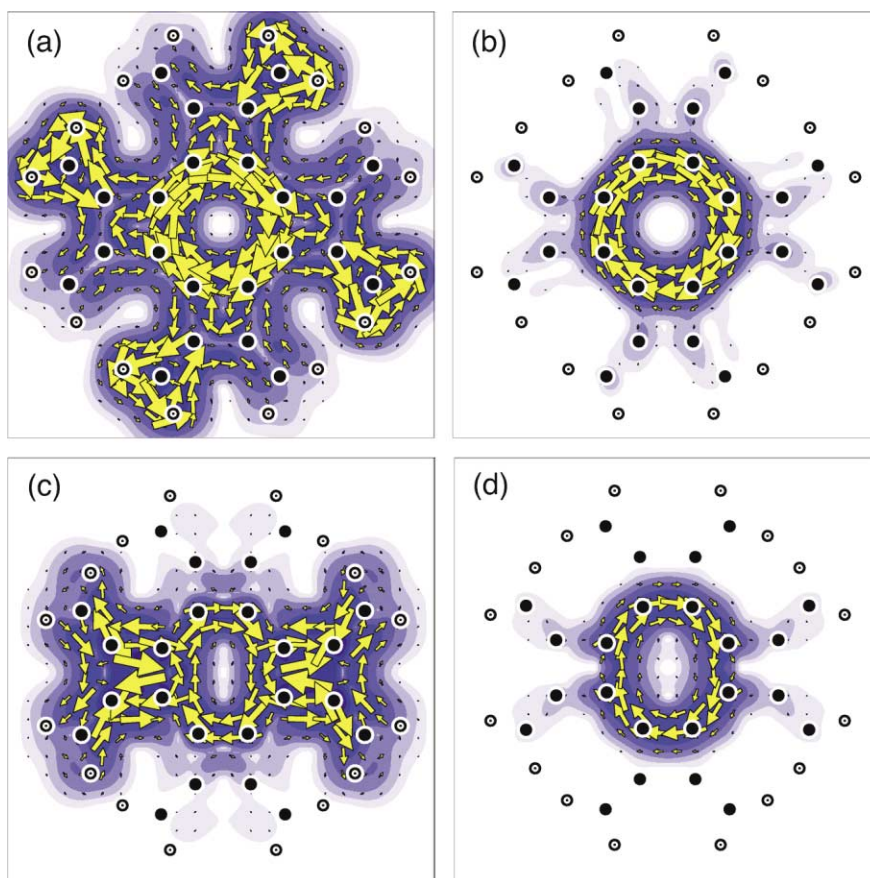


Fig. 4 CTOCD-DZ/6-31G**//RHF/6-31G** current density maps for two local minima, *exo-10b* (D_4) and *endo-9c* (D_{2d}); (a) total for *exo-10b*, (b) $11b_1$ HOMO contribution in *exo-10b*, (c) total of *endo-9c* (a cut-off of 0.1 was applied to remove the large arrows where bonds are cut by the plotting plane) and (d) $12a_1$ HOMO contribution in *endo-9c*: carbon ● and hydrogen ○.

electronic structure and does not support a ring current,⁸ but in the present case the deviation from planarity is smaller [RHF/6-31G** $d_{\text{plane...plane}}$ 0.41 Å (**9c**) and 0.76 Å (free COT)⁸] and π -orbital overlap is evidently sufficient to maintain delocalisation.

The main conclusion from the maps of clamped benzene and COT systems is that the *unsaturated* 3,4-dimethylenecyclobuteno moiety acts in the same way as the *saturated* cyclobutano-group (Scheme 1). The two groups impose a similar degree of bond alternation on benzene (Table 1). Likewise, although the steric bulk of the 3,4-dimethylenecyclobuteno clamp prevents complete flattening of COT, bond alternation effects in the two clamped COT systems are similar (Table 1). Both clamps are similarly *ineffective* in changing the diatropic character of benzene and the paratropic character of planar COT. Thus, although the 3,4-dimethylenecyclobuteno moiety is unsaturated, it is behaving much as if it were a saturated clamp. The challenge is to reconcile this with the existing orbital-based rationale.

Discussion

From *ab initio* calculated maps we now have examples of two distinct types of unsaturated clamping group: the cyclobutadieno clamp, which quenches the monocycle currents,^{7,8} and the 3,4-dimethylenecyclobuteno clamp, which does not. In fact, the qualitative difference between them can be understood easily in terms of pictorial molecular-orbital arguments.

First consider the cyclobutadieno clamp in **4**. Attachment of three clamps imposes D_{3h} symmetry on the hexagonal monocycle and in this point group the π orbitals of benzene span $a_1'' + a_2'' + 2e''$, so that its HOMO and LUMO become *equisymmetric* in the lowered symmetry. The cyclobutadieno clamps contribute a second copy of $a_1'' + a_2'' + 2e''$. Interaction produces a new π system in which every molecular orbital contains

symmetry-matched contributions from clamps and the central ring. A correlation diagram for the composite system can be constructed by taking a formal starting point of three ethenes and one benzene and allowing the resonance parameter for the six connecting carbon-carbon bonds to grow smoothly from 0 to its full value β . This reveals the salient features of the frontier π molecular orbitals in **4**: the HOMO of **4** belongs to the non-degenerate a_2'' symmetry and is formed by *out-of-phase* combination of the lowest π orbital of benzene and the π bonding orbitals of the three ethene moieties [Fig. 5 (a)]. The original HOMO of benzene contributes not to the HOMO of the composite system, but to the e'' HOMO-1 pair, where it is in near-equal admixture with the original LUMO of benzene and with bonding/anti-bonding orbitals of the three ethenes [Fig. 5 (b)]. Thus, the HOMO of **4** is the combination

$$0.53\psi_1[a_2''] - 0.85\psi_2[a_2'']$$

of the (normalised) basis functions on inner ($i = 1$) and outer ($i = 2$) sets of carbon centres,

$$\psi_i[a_2''] \sim \{+1, +1, +1, +1, +1, +1, +1\}$$

The HOMO-1 pair of **4** is a strong mixture of HOMO and LUMO of the central ring, containing near-equal amounts of basis functions

$$\psi_i[1e''] \sim \{+1, +1, 0, -1, -1, 0\}, \sim \{+1, +1, +2, -1, -1, -2\}$$

and

$$\psi_i[2e''] \sim \{+1, -1, 0, +1, -1, 0\}, \sim \{+1, -1, +2, +1, -1, +2\}$$

(respectively central HOMO and central LUMO when $i = 1$) in the combination

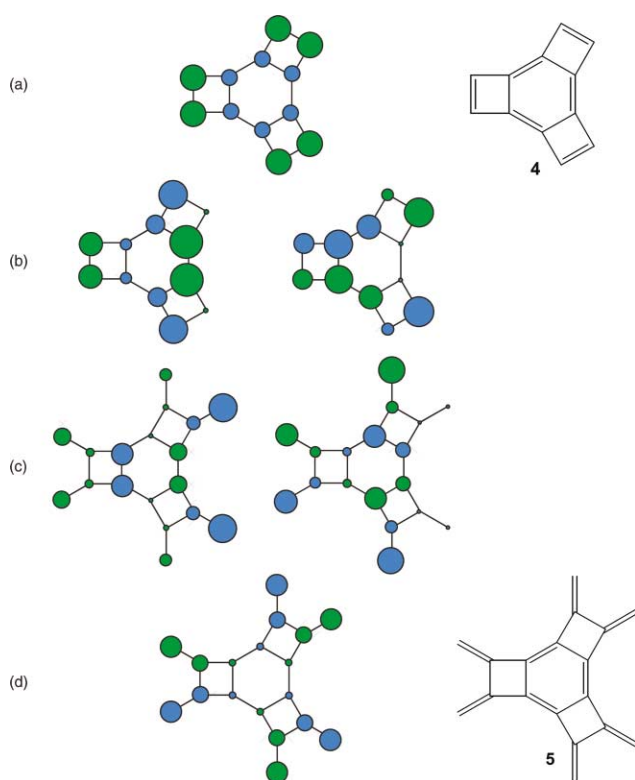


Fig. 5 Hückel frontier bonding orbitals for the clamped benzenes **4** and **5** (see also Scheme 1).

$$-0.56\psi_1[1e''] + 0.43\psi_1[2e''] + 0.27\psi_2[1e''] + 0.65\psi_2[2e'']$$

As the system remains an *alternant* at all stages of the interaction, the compositions of a_1'' LUMO and e'' LUMO + 1 orbitals follow by reversing relative signs of coefficients on the two sets of centres composing this bipartite graph.

Thus, the separate identity of the benzene frontier orbitals is lost in this clamped system and the dominant occupied-to-virtual transitions are no longer simple monocycle HOMO–LUMO transitions. According to the ipsocentric approach the monocycle ring current can be expected to be quenched, as is indeed found to be the case in explicit *ab initio* calculations.⁹ At the RHF/6-31G** level, $2a_2''$ and $2e''$ are still almost isoenergetic with $2a_2''$ moving to just below $2e''$, and $1a_1''$ and $3e''$ stay as LUMO and LUMO + 1, respectively. The composition of the frontier orbitals, and therefore the explanation of ring-current activity, remains as described at the Hückel level (see Fig. 2 of reference 7).

In contrast, with the 3,4-dimethylenecyclobuteno clamp, the composite π system (**5**) spans three copies of the symmetry $a_1'' + a_2'' + 2e''$, and the orbitals can be formally derived from the interaction of a benzene unit with three butadiene moieties. The e'' HOMO pair in the clamped system contains a benzene-like HOMO on the central ring, only lightly contaminated by the benzene LUMO and combined in *anti*-bonding fashion with butadiene bonding orbitals [Fig. 5 (c)].

With basis functions defined as above for the inner, middle and outer sets of six equivalent carbon centres ($i = 1,2,3$), the HOMO pair of **5** is the combination

$$-0.57\psi_1[1e''] - 0.10\psi_1[2e''] + 0.31\psi_2[1e''] - 0.14\psi_2[2e''] \\ + 0.68\psi_3[1e''] - 0.31\psi_3[2e'']$$

and the a_1'' frontier orbital of **5** is an in-phase combination of the fully antibonding combinations on all three sets of six centres:

$$+0.21\psi_1[a_1''] + 0.58\psi_2[a_1''] + 0.79\psi_3[a_1'']$$

with

$$\psi_1[a_1''] \sim \{+1, -1, +1, -1, +1, -1\}.$$

The contributions from the orbitals of the butadiene moieties (*i.e.*, middle and outer sets of carbon centres) to HOMO and LUMO of **5** are large, but as these frontier orbitals have a close local match on the central ring to those of benzene [Fig. 5 (d)], the transition integrals governing central ring current will be similar to those in the unperturbed monocycle. Thus, the monocycle ring current will persist, as is indeed found to be the case in the *ab initio* calculations described above.

Similar reasoning applies to the interactions of the two different π clamps with COT. The strong paratropic current in planar COT arises from the rotationally allowed transition across the small energy gap between the $b_{2u} + b_{1u}$ HOMO–LUMO pair.⁸ Clamping with four cyclobutadieno units (*exo*-**8**) leads to orbital reordering and quenching of the current, whereas the system with four 3,4-dimethylenecyclobuteno clamps (*endo*-**9a** and *exo*-**10a**) retains the native COT frontier-orbital symmetries and, hence, the paratropic current.

Conclusions

This simplified model of the π clamped species as interacting polyene + monocycle systems shows the key to the difference between the two types of π clamp. The difference lies in the *topological* match or mismatch between frontier orbitals of the incoming polyene moiety and those of the central monocycle. In the case of ethene, the single π bonding orbital of the clamp presents *in-phase* centres to the benzene of **4**; no combination of in-phase ethene HOMO's can match the HOMO of benzene. When the incoming polyene is butadiene, the highest occupied orbital presents an *out-of-phase* pair to benzene in **5** and, hence, a mixture of occupied orbitals that can match the benzene HOMO. Thus, the essential difference between the π clamps is one of *parity*. Many predictions concerning the ring current effects of polyene clamps of varying lengths and positions of attachment follow as direct corollaries. In particular, **4** and **5**, and likewise their COT analogues, can be seen as the first two members of a series in which quenching and survival of ring currents is modulated by the odd or even number of the atoms in the symmetrically placed clamping polyene.

Note that this explanation of quenching/survival of current is logically independent of the degree of bond alternation in the clamped monocycle. Ring currents are known to be remarkably robust against pure geometrical change,¹⁰ and indeed the pictorial molecular orbital model^{1,2} does predict alternation of bond order, and hence bond length, in the clamped monocycles: the alternation in π bond order is stronger for **4** and **8**, and weaker for **5** and **9/10**, with consequences for their geometries that are qualitatively consistent with the full *ab initio* results. Although there is a history of discussion in the literature of the origin, direction and extent of bond alternation in clamped π -conjugated systems, *i.e.* the Mills–Nixon effect,⁶ our point here is that changes in ring current are *not* primarily caused by the geometrical changes; both are consequences of electronic structure. The key to the understanding of the effects of σ and π clamps, and to the differential effects of different π clamps, lies in the nature of the frontier orbitals.

Acknowledgements

The authors acknowledge financial support from the EU Framework V programme (RTN Contract HPRN-CT-2002-00136 'WONDERFULL'; A. S.) and the International Author Travel Grant programme of the Royal Society of Chemistry (0301433; L. W. J.).

References

- 1 E. Steiner and P. W. Fowler, *Chem. Commun.*, 2001, 2220–2221.
- 2 E. Steiner and P. W. Fowler, *J. Phys. Chem. A*, 2001, **105**, 9553–9562.
- 3 R. Diercks and K. P. C. Vollhardt, *J. Am. Chem. Soc.*, 1986, **108**, 3150–3152.
- 4 H.-B. Bürgi, K. K. Baldrige, K. Hardcastle, N. L. Frank, P. Gantzel, J. S. Siegel and J. Ziller, *Angew. Chem.*, 1995, **107**, 1575–1577; H.-B. Bürgi, K. K. Baldrige, K. Hardcastle, N. L. Frank, P. Gantzel, J. S. Siegel and J. Ziller, *Angew. Chem., Int. Ed.*, 1995, **34**, 1454–1456.
- 5 A. Matsuura and K. Komatsu, *J. Am. Chem. Soc.*, 2001, **123**, 1768–1769.
- 6 For different views on the Mills–Nixon effects see: (a) W. H. Mills and I. G. Nixon, *J. Chem. Soc.*, 1930, 2510–2524; (b) A. Stanger, *J. Am. Chem. Soc.*, 1991, **113**, 8277–8280; (c) K. K. Baldrige and J. S. Siegel, *J. Am. Chem. Soc.*, 1992, **114**, 9583–9587; (d) A. Stanger, *J. Am. Chem. Soc.*, 1998, **120**, 12034–12040; (e) Z. B. Maksić, M. Eckert-Maksić, O. Mó and M. Yáñez, *Pauling's Legacy—Modern Modelling of the Chemical Bond*, eds. Z. B. Maksić and W. J. Orville–Thomas, Elsevier, Amsterdam, The Netherlands, 1999, p. 47; and references cited; (f) A. Stanger and E. Tkachenko, *J. Comput. Chem.*, 2001, **22**, 1377–1386 and references cited.
- 7 P. W. Fowler, R. W. A. Havenith, L. W. Jenneskens, A. Soncini and E. Steiner, *Chem. Commun.*, 2001, 2386–2387.
- 8 P. W. Fowler, R. W. A. Havenith, L. W. Jenneskens, A. Soncini and E. Steiner, *Angew. Chem.*, 2002, **114**, 1628–1630; P. W. Fowler, R. W. A. Havenith, L. W. Jenneskens, A. Soncini and E. Steiner, *Angew. Chem., Int. Ed.*, 2002, **41**, 1558–1560.
- 9 A. Soncini, R. W. A. Havenith, P. W. Fowler, L. W. Jenneskens and E. Steiner, *J. Org. Chem.*, 2002, **67**, 4753–4758.
- 10 R. W. A. Havenith, L. W. Jenneskens and P. W. Fowler, *Chem. Phys. Lett.*, 2003, **367**, 468–474 and references cited.
- 11 R. Faust, E. D. Glendening, A. Streitwieser and K. P. C. Vollhardt, *J. Am. Chem. Soc.*, 1992, **114**, 8263–8268.
- 12 J. M. Schulman, R. L. Disch, H. Jiao and P. von R. Schleyer, *J. Phys. Chem. A*, 1998, **102**, 8051–8055.
- 13 M. F. Guest, J. H. van Lenthe, J. Kendrick, K. Schöffel, P. Sherwood, R. J. Harrison, GAMESS-UK, a package of *ab initio*, programs, 2002, with contributions from R. D. Amos, R. J. Buenker, H. J. J. van Dam, M. Dupuis, N. C. Handy, I. H. Hillier, P. J. Knowles, V. Bonacic-Koutecky, W. von Niessen, R. J. Harrison, A. P. Rendell, V. R. Saunders, A. J. Stone, D. J. Tozer, A. H. de Vries. It is derived from the original GAMESS code due to M. Dupuis, D. Spangler, J. Wendolowski, *NRCC Software Catalog, Vol. 1*, Program No. QG01 (GAMESS), 1980.
- 14 K. K. Baldrige and J. S. Siegel, *J. Am. Chem. Soc.*, 2002, **124**, 5514–5517.
- 15 A. Keith and R. F. W. Bader, *Chem. Phys. Lett.*, 1993, **210**, 223–231; A. Keith and R. F. W. Bader, *J. Chem. Phys.*, 1993, **99**, 3669–3682; S. Coriani, P. Lazzeretti, M. Malagoli and R. Zanasi, *Theor. Chim. Acta*, 1994, **89**, 181–192; R. Zanasi, *J. Chem. Phys.*, 1996, **105**, 1460–1469.
- 16 P. Lazzeretti, R. Zanasi, SYSMO package (University of Modena), 1980, with additional routines for evaluation and plotting of current density by E. Steiner, P. W. Fowler (Univ. of Exeter, UK), unpublished results.
- 17 A. Ligabue and P. Lazzeretti, *J. Chem. Phys.*, 2002, **116**, 964–973.